

Article

COVID-19 Active Case Forecasts in Latin American Countries Using Score-Driven Models

Sergio Contreras-Espinoza ^{1,*}, Francisco Novoa-Muñoz ¹, Szabolcs Blazsek ², Pedro Vidal ¹
and Christian Caamaño-Carrillo ¹

¹ Departamento de Estadística, Facultad de Ciencias, Universidad del Bío-Bío, Concepción 4081112, Chile

² Escuela de Negocios, Universidad Francisco Marroquín, Guatemala City 01011, Guatemala

* Correspondence: scontre@ubiobio.cl; Tel.: +56-9-75873480

Abstract: With the aim of mitigating the damage caused by the coronavirus disease 2019 (COVID-19) pandemic, it is important to use models that allow forecasting possible new infections accurately in order to face the pandemic in specific sociocultural contexts in the best possible way. Our first contribution is empirical. We use an extensive COVID-19 dataset from nine Latin American countries for the period of 1 April 2020 to 31 December 2021. Our second and third contributions are methodological. We extend relevant (i) state-space models with score-driven dynamics and (ii) nonlinear state-space models with unobserved components, respectively. We use weekly seasonal effects, in addition to the local-level and trend filters of the literature, for (i) and (ii), and the negative binomial distribution for (ii). We find that the statistical and forecasting performances of the novel score-driven specifications are superior to those of the nonlinear state-space models with unobserved components model, providing a potential valid alternative to forecasting the number of possible new COVID-19 infections.

Keywords: COVID-19; score-driven models; unobserved components; negative binomial distribution

MSC: 37M10; 46N30



Citation: Contreras-Espinoza, S.; Novoa-Muñoz, F.; Blazsek, S.; Vidal, P.; Caamaño-Carrillo, C. COVID-19 Active Case Forecasts in Latin American Countries Using Score-Driven Models. *Mathematics* **2023**, *11*, 136. <https://doi.org/10.3390/math11010136>

Academic Editor: Alexander B. Medvinsky

Received: 6 November 2022

Revised: 29 November 2022

Accepted: 2 December 2022

Published: 27 December 2022



Copyright: © 2022 by the authors. Licensee MDPI, Basel, Switzerland. This article is an open access article distributed under the terms and conditions of the Creative Commons Attribution (CC BY) license (<https://creativecommons.org/licenses/by/4.0/>).

1. Introduction

In the work of Barrado [1], the author presents that the sanitary (health) crisis produced by the coronavirus disease 2019 (COVID-19) pandemic generated by the Sars-CoV-2 (severe acute respiratory syndrome coronavirus 2) is not the first zoonotic disease (i.e., rabies in the seventeenth century; 1918 influenza pandemic; pandemic of AIDS/HIV—acquired immune deficiency syndrome/human immunodeficiency virus—infection of 1981 to date) and, unfortunately, it will not be the last that humanity will face. Diseases, in fact, have been powerful levers of historical change; they have the ability to change a society.

The plagues in Egypt (1570 to 1440 BC, before Christ) caused notable changes in the way of life of the population, since they affected the characteristics of social relations [2]. The Black Death, a pandemic that ravaged Europe between 1347 and 1351, gave rise to an epidemic reaching all the European continent geographically, causing the death of about one-third of its population [3] and changing its socioeconomic structure. The encounter between Europeans and Native Americans (1770s to 1850) caused epidemics that devastated the native society, being one of the main causes of the destruction of their culture [4]. In all three examples, for both political structures and individuals involved, the changes were dramatic and left multiple victims, but new opportunities were also opened up.

During the emergence of the modern states, statistics began to be used to know precisely the forces of the state, starting with the birth, mortality, and disease records. In this way, the health statistics kept an accurate record of the cases of illness and death of the population emerged. Those records made possible the study of epidemic phenomena by

using modern scientific tools [5]. The work of [6] presents models to predict the evolution of the COVID-19 pandemic and the impact of the measures for its control. The work of [7] also presents that there are many models developed to understand the dynamics of the COVID-19 disease. However, the different sociocultural contexts of different countries make it necessary to specifically adjust those models to each scenario [7]. The first contribution of our paper is empirical. To the best of our knowledge, our paper provides the most complete analysis on COVID-19 forecasting for Latin American countries in the literature. We study the forecasting performances of new time series models in the sociocultural contexts of nine Latin American countries for the period of April 2020 to December 2021. In Table A1 of Appendix A, we cite several works from the literature on COVID-19 forecasting.

In the present paper, we use two classes of time series models for COVID-19 forecasting. For the first class of time series models, we use score-driven models which are introduced in the works of [8,9]. In those papers, score-driven models are named generalized autoregressive score (GAS) and dynamic conditional score (DCS) models, respectively. Score-driven models are observation-driven state-space models [10], in which the dynamic parameters are observable and updated by past observations. For reviews on score-driven models, we refer to [11,12]. For the statistical inference of score-driven models, we refer to the works of [11,13–19]. From the literature, the most relevant works for us are [20,21], in which one of the models for the log of new COVID-19 cases is a score-driven model for the negative binomial distribution using score-driven local-level and trend components. The second contribution of our paper, in relation to score-driven models, is methodological. We extend the works of [20,21] by adding a weekly seasonal component for new COVID-19 cases. In addition, we also refer to relevant works in which score-driven seasonal components are used for macroeconomic data: [22–26].

For the second class of time series models, we use space-state models with unobserved components [11,27–30], which are also called structural models [30]. The most relevant papers for us are [20,21], in which one of the models for the log of new COVID-19 cases is a Gaussian linear state-space model with unobserved components of local level and trend. The third contribution of our paper, in relation to state-space models with unobserved components, is methodological. We extend the state-space model with unobserved components of [20,21] at two points: (i) We add a weekly seasonal component for new COVID-19 cases that we observe at the daily frequency. (ii) We assume that the data-generating process (DGP) for the state-space model with unobserved components is the negative binomial distribution, and we use the estimation method of [31]. The use of the negative binomial distribution is motivated by the works of [20,21] due to robustness to possible small numbers of new COVID-19 cases in the data series.

By using the new state-space model with unobserved components for the negative binomial distribution, we separately model the trend, seasonality, and seasonal components of new COVID-19 cases, and we study the out-of-sample forecasting accuracy for COVID-19 cases using alternative forecasting horizons. Our estimation results indicate that the COVID-19 forecasting performances of the score-driven models are superior to those of the state-space models with unobserved components.

In the remainder of this paper, Section 2 presents the statistical models, Section 3 presents the results, and Section 4 concludes.

2. Materials and Methods

We use COVID-19 data from Latin American countries for which data are available to us, and we discuss in detail the results for Chile. The first cases of the COVID-19 pandemic in Chile were confirmed on 3 March 2020, when a 33-year-old man from the commune of San Javier (Maule Region) and a passenger of a flight from Singapore were hospitalized in the Regional Hospital of Talca [32]. From these first proven cases, the epidemic outbreak spread to sixteen regions of the country. By April 2020, Chile was the country that performed the most PCR (polymerase chain reaction) tests per million inhabitants in Latin America.

The data of the present paper are from the COVID-19 Data Repository of the Center for Systems Science and Engineering (CSSE) at Johns Hopkins University [33] for the period of 1 April 2020 to 31 December 2021 of nine Latin American Countries for which daily data were available in the study period. For the data under study, various specifications of state-space models with unobserved components and score-driven models are estimated, and in-sample model fits are compared.

Out-of-sample forecasts of COVID-19 cases are also performed for the alternative forecasting windows of 7, 14, and 28 days. By evaluating the alternative state-space models, we find that the in-sample statistical and out-of-sample forecasting performances of a score-driven model with dynamic local-level, trend, and seasonal components are superior to those of the nonlinear state-space model with unobserved components. The novel score-driven model may be used to decide on alternative actions, such as quarantines and vaccination processes, to control the current COVID-19 or other future pandemics.

Next, we present the score-driven model of location, trend, and seasonality for the negative binomial distribution. Then, we review the corresponding nonlinear state-space model for the same probability distribution.

2.1. Score-Driven Models

In the score-driven models of new COVID-19 cases of the present paper, the score-driven parameter f_t and the constant parameters of the vector Θ influence the conditional density of the dependent variable $y_t \sim p_y(y_t|y_1, \dots, y_{t-1}, f_t, \Theta)$, where y_t denotes the number of new COVID-19 cases in period t . Similar to the work of [20], we assume that the DGP for new COVID-19 cases is the negative binomial distribution. Hence, the conditional density of y_t is defined in Equation (1) next,

$$p(y_t|y_1, \dots, y_{t-1}, f_t, \Theta) = \frac{\Gamma(v + y_t)}{y_t! \Gamma(v)} f_t^{y_t} (v + f_t)^{-y_t} (1 + f_t/v)^{-v}, \tag{1}$$

where $\Gamma(x)$ is the gamma function, $n! = (1 \times 2 \times \dots \times n)$ denotes factorial, v is the shape parameter, the conditional mean of new COVID-19 cases is $E(y_t|y_1, \dots, y_{t-1}) = f_t$, the conditional variance of new COVID-19 cases is $Var(y_t|y_1, \dots, y_{t-1}) = f_t + (f_t^2)/v$, and the dynamics of $\ln f_t$ are driven as formulated in Equations (2)–(7) follows:

$$\ln f_t = \delta_t + s_t \tag{2}$$

$$\delta_t = \delta_{t-1} + \beta_{t-1} + \kappa_1 u_{t-1} \tag{3}$$

$$\beta_t = \beta_{t-1} + \kappa_2 u_{t-1} \tag{4}$$

$$s_t = D_t \gamma_t \tag{5}$$

$$D_t = (D_{\text{Monday},t}, \dots, D_{\text{Sunday},t}) \tag{6}$$

$$\gamma_t = \gamma_{t-1} + \kappa_t u_{t-1} \tag{7}$$

where δ_t (1×1) is the local level component, β_t (1×1) is the trend component, and s_t (1×1) is the seasonality component. The score-driven model can be extended by adding strictly exogenous variables to Equation (2) ([11], p. 56), which influence the new cases of COVID-19. Moreover, γ_t is a (7×1) vector of seasonality filter, where its elements are of the form of Equation (8):

$$\gamma_t = (\gamma_{\text{Monday},t}, \dots, \gamma_{\text{Sunday},t})^\top, \tag{8}$$

where κ_t is a (7×1) vector, where each element of κ_t is parameterized as in Equation (9):

$$\kappa_{j,t} = \begin{cases} \kappa_j, & \text{if } D_{j,t} = 1; \\ -\frac{\kappa_j}{7-1}, & \text{if } D_{j,t} = 0. \end{cases} \tag{9}$$

where $j \in \{\text{Monday, Tuesday, } \dots, \text{Sunday}\}$. Hence, parameters κ_j where $j \in \{\text{Monday, Tuesday, } \dots, \text{Sunday}\}$ are time-invariant parameters which are jointly estimated with the rest of the parameters. Finally, the conditional score of the log-likelihood with respect to f_t (i.e., score function) is given by Equation (10):

$$\frac{\partial \ln p(y_t|y_1, \dots, y_{t-1}, f_t, \Theta)}{\partial f_t} = \frac{v(y_t - f_t)}{f_t(v + f_t)}. \tag{10}$$

In the literature on score-driven models (e.g., [11,13]), in many cases, the conditional score is scaled by the inverse information matrix. Hence, following the work of [20], the scaled score function updating term in Equations (3), (4) and (7) is given by $u_t = y_t / f_t - 1$, which is the score function divided by the information quantity.

We consider alternative specifications of the general score-driven model of this section; the specification presented in this section is denoted by SD 1 (score-driven 1). An alternative specification assumes that all seasonality parameters are identical, i.e., $\kappa_j = \kappa$ for all j , which we denote by SD 2 (score-driven 2). Moreover, another alternative specification assumes that only local-level and trend components are included in the model, i.e., $s_t = 0$ for $t = 1, \dots, T$. We denote the latter specification by SD WS (score-driven, without seasonality), which coincides with the score-driven models of [20,21].

2.2. State-Space Model

We use the exponential family state-space model and apply it to the negative binomial distribution, as seen in the work of [31]. We use the same conditional density for y_t as for the score-driven model; see Equation (1). The estimation method uses a Gaussian model which approximates the negative binomial model. Then, the estimation is performed by using the Kalman filter procedure. The log-mean of y_t is formulated by Equations (11)–(17):

$$\ln f_t = \delta_t + s_t \tag{11}$$

$$\delta_t = \delta_{t-1} + \beta_{t-1} + \epsilon_{\delta,t} \tag{12}$$

$$\beta_t = \beta_{t-1} + \epsilon_{\beta,t} \tag{13}$$

$$s_t = D_t \gamma_t \tag{14}$$

$$D_t = (D_{\text{Monday},t}, \dots, D_{\text{Sunday},t}) \tag{15}$$

$$\gamma_t = \gamma_{t-1} + \epsilon_{\gamma,t} \tag{16}$$

$$\epsilon_{\gamma,t} = (\epsilon_{\text{Monday},\gamma,t}, \dots, \epsilon_{\text{Sunday},\gamma,t})' \tag{17}$$

where δ_t (1×1) is the local level component, β_t (1×1) is the trend component, s_t (1×1) is the seasonality component, and γ_t (7×1) is the seasonality filter of time-varying parameters. We assume that $\epsilon_{\delta,t} \sim N(0, \sigma_\delta^2)$ and $\epsilon_{\beta,t} \sim N(0, \sigma_\beta^2)$. Moreover, we also assume that $\epsilon_{\gamma,t}$ has a seven-dimensional multivariate normal distribution where the mean is a zero vector and the variance is specified as follows: $\text{Var}(\epsilon_{\gamma,t}) = \sigma_\gamma^2 (I_7 - (1/7) i_7 i_7')$ where I_7 is the identity matrix and i_7 is a (7×1) vector of ones. This specification of the covariance matrix ensures that the sum of each column of that matrix is zero, i.e., the sum of the seasonality filters is zero in each period. The nonlinear state-space model with unobserved components for the negative binomial distribution of this section is denoted SS (state-space).

2.3. Parameter Estimation and Statistical Performance

All models are estimated by using the maximum likelihood (ML) method, in which the following log-likelihood (LL) function is maximized with respect to the parameter vector Θ as is defined in (18):

$$\hat{\Theta} = \text{argmax}_{\Theta} \text{LL}(y_1, \dots, y_T, \Theta) = \text{argmax}_{\Theta} \sum_{t=1}^T \ln p(y_t|y_1, \dots, y_{t-1}, f_t, \Theta). \tag{18}$$

For the estimation of the nonlinear state-space model, we refer to the work of [31]. For the estimation of the score-driven model, we refer to the works of [11,13,14].

The statistical performances of different models are compared by using the following likelihood-based model performance metrics defined as Equations (19)–(21):

$$AIC = 2K - 2\hat{L}L \tag{19}$$

$$AICc = AIC + \frac{2K^2 + 2K}{T - K - 1} \tag{20}$$

$$BIC = K \ln(T) - 2\hat{L}L \tag{21}$$

where $\hat{L}L$ is the maximum value of the log-likelihood, K is the number of time-invariant parameters, and T denotes the sample size. Moreover, AIC denotes Akaike information criterion, AICc is a corrected AIC which is robust to small sample size, and BIC denotes Bayesian information criterion. The use of these model selection metrics for score-driven models is motivated by the work of [11] (p. 56).

3. Results

To evaluate the in-sample and out-of-sample performances of the models, a time series of new daily infections of COVID-19 in nine Latin American countries, for the period of 1 April 2020 to 31 December 2021, with a total of $T = 640$ observations, is considered [33]. Table 1 presents summary statistics of the data and the p -values of the Jarque–Bera (JB) [34] and augmented Dickey–Fuller (ADF) tests [35]. For the JB test, the null hypothesis of normal distribution is rejected for all countries at the 1% level of significance. This supports the use of the negative binomial distribution for the score-driven model. For the ADF test, the null hypothesis of unit root process cannot be rejected for any of the countries, which supports the use of the unit root specifications for δ_i in Equations (3) and (12).

Table 1. Descriptive statistics, JB test, and ADF test for new COVID-19 cases.

	Mean	SDev	Minimum	Maximum	Skewness	Kurtosis	JB p -Value	ADF p -Value
Argentina	8833.3656	8478.1008	0.0000	50,506.0000	1.5262	5.6897	0.0000	0.8786
Brazil	10,490.3422	9139.8157	0.0000	63,523.0000	1.6401	6.6768	0.0000	0.5559
Chile	2820.9703	2168.6074	265.0000	13,990.0000	1.2857	4.6445	0.0000	0.7233
Colombia	8057.0844	7314.7682	67.0000	33,594.0000	1.2759	4.2166	0.0000	0.6428
Cuba	1509.0906	2618.5288	0.0000	9907.0000	1.9932	5.5462	0.0000	0.8492
Guatemala	981.7516	1090.4835	0.0000	5826.0000	2.0654	7.0469	0.0000	0.9058
Jamaica	146.6938	190.1864	0.0000	1430.0000	2.2203	8.8093	0.0000	0.4927
Panama	765.6219	723.4916	0.0000	5186.0000	2.4510	10.8399	0.0000	0.5985
Uruguay	645.6234	1072.7704	0.0000	7289.0000	2.2389	8.0831	0.0000	0.8074

For the full sample period, parameter estimates for SD 1, SD2, SD WS, and SS are reported in Tables A2–A10 of Appendix B for all countries. To evaluate the predictive capacity, first, the sample was divided into two equal parts, each of 320 observations. The last 7, 14, and 28 observations were removed from the initial half of the data, which were predicted using the fitted model for the remaining data, and measures were calculated to evaluate the predictive capacity of the models considered. Then, the next observation was included, having now a total of 321 observations. Again, the last 7, 14, and 21 final observations were removed, the prediction of these was made and measurements of the quality of the prediction quality were calculated. The procedure described above was repeated until the total set of available observations was considered.

In Figure 1 (graph of the analyzed time series of Chile), it is possible to see five periods of significant increase in the number of new cases of infection with COVID-19.

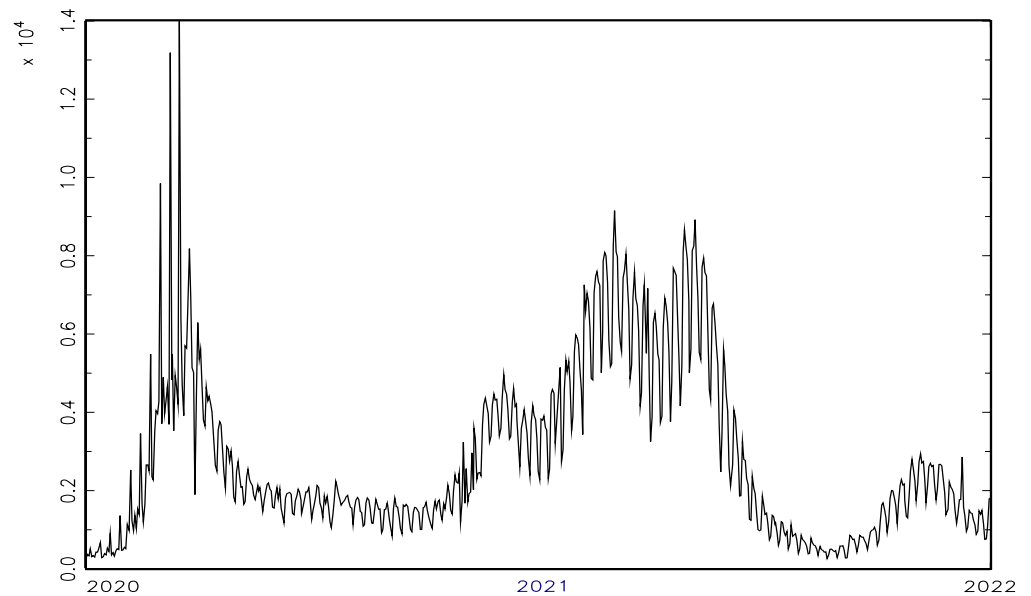


Figure 1. New cases of infection with COVID-19 in Chile (1 April 2020 to 31 December 2021).

The quality of predictions is compared by using the following mean absolute percentage error (MAPE), mean absolute error (MAE), and mean square error (MSE) loss functions presented in Equations (22)–(24).

$$\text{MAPE} = \frac{1}{T} \sum_{t=1}^T \frac{|y_t - y_{f,t}|}{y_t} \tag{22}$$

$$\text{MAE} = \frac{1}{T} \sum_{t=1}^T |y_t - y_{f,t}| \tag{23}$$

$$\text{MSE} = \frac{1}{T} \sum_{t=1}^T (y_t - y_{f,t})^2 \tag{24}$$

The precision of the forecasts is studied for models SD 1, SD 2, SD WS, and SS.

Table 2 shows the mean values of AIC, AICc, BIC, MSE, MAE, and MAPE of different models for the estimation window of the countries used in the present study by excluding the last seven observations, which are used to evaluate the predictive capacity of the models in question. Table 3 also presents the same results when the last 14 observations were excluded from the sample. Table 4 presents similar result for the estimation window by excluding the last 28 observations which are used to evaluate the predictive capacity of the models in question.

According to the tables, in which the best values have been highlighted in bold, the SD 1 or SD 2 model has a superior performance according to all in-sample model performance metrics and out-of-sample loss functions. Furthermore, when the prediction horizon increases, the prediction quality values decrease, and in the particular case of Chile, the values of MAPE is 12.4% for the forecast by the next seven days, 16.2% by 14 days and 26.8% by 28 days. The other countries present similar conducts.

Figure 2 shows the 28-day ahead forecasts for SD 1. The filtered estimate of f_t and the 28-day out-of-sample ahead forecast $y_{f,t}$ are presented. The thick red line indicates the forecasting period for this example. The figures for the other econometric models of this paper are similar and are available from the authors upon request. When comparing Figures 1 and 2, it can be seen that the prediction is close to the real value and the fit follows the behavior of the data.

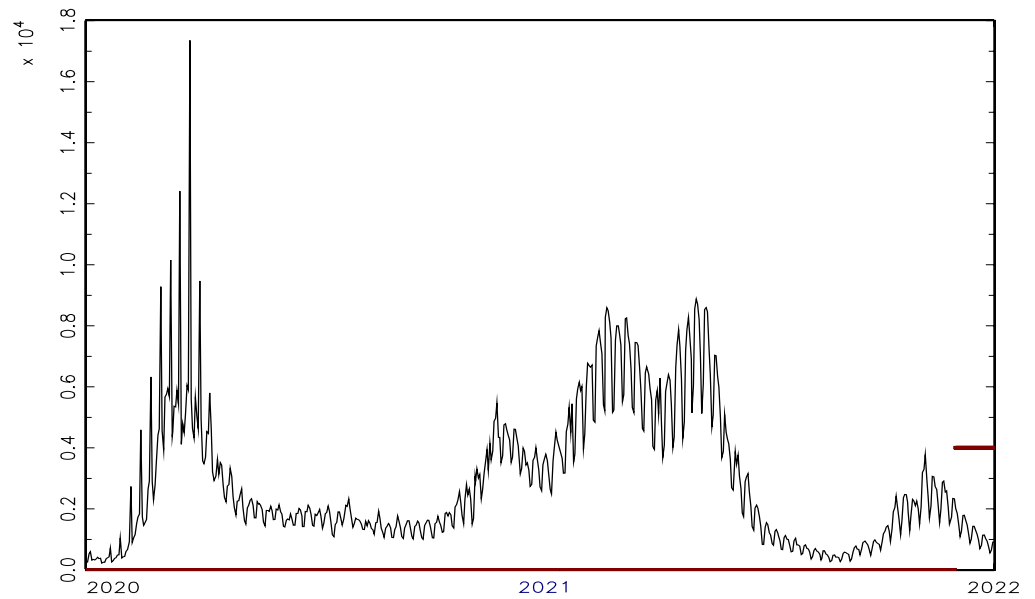


Figure 2. Filtered estimates and forecasts of new cases of infection with COVID-19 in Chile (1 April 2020 to 31 December 2021). *Note:* The thick red line indicates the forecasting period for this example.

Table 2. AIC, AICc, BIC, and loss functions (forecasting window: last 7 days).

Country	Model	AIC	AICc	BIC	MSE	MAE	MAPE
Argentina	SD 1	8296.3733	8297.9455	8370.9011	2301.2016	1946.0298	18.8640
	SD 2	8377.7886	8378.4967	8427.4559	2316.1415	1974.9102	19.0833
	SD WS	8535.3791	8535.5133	8556.0693	34,343,289.6112	3551.2989	40.0326
	SS	8498.8841	8499.3802	8540.2884	13,108,686.9670	2017.2896	22.0692
Brazil	SD 1	8768.5371	8770.1093	8843.0649	2274.6951	1911.7838	19.9625
	SD 2	8767.4572	8768.1673	8817.0885	2602.3998	2228.8968	22.7865
	SD WS	8534.4407	8534.5821	8554.8778	42,251,093.3462	4151.6625	49.4397
	SS	8998.2551	8998.7500	9039.6803	16,851,638.8005	2361.7759	25.4773
Chile	SD 1	7001.2412	7002.8134	7075.7690	415.3421	339.2591	12.4051
	SD 2	7049.7117	7050.4198	7099.3798	405.6187	336.4485	12.2171
	SD WS	7492.7113	7492.8451	7513.4124	749,400.2033	622.5042	22.9498
	SS	7097.0747	7097.5709	7138.4791	348,105.9045	414.0706	16.4325
Colombia	SD 1	7775.4984	7776.2069	7825.1567	1499.3427	1306.5852	14.8406
	SD 2	7748.3902	7749.9624	7822.9179	1467.6770	1292.4946	14.4201
	SD WS	7854.5344	7854.6684	7875.2237	6,187,717.7639	1472.9147	16.4635
	SS	7833.7131	7834.2092	7875.1174	5,658,909.4517	1473.1866	17.9121
Cuba	SD 1	5194.5309	5196.1031	5269.0587	523.5462	464.6705	19.5876
	SD 2	5233.4356	5234.1439	5283.0955	699.1034	637.0687	21.9416
	SD WS	5192.3540	5192.4877	5213.0588	1,546,392.2398	563.7378	18.7016
	SS	5032.0991	5032.5952	5073.5034	641,855.0899	454.5395	21.3560
Guatemala	SD 1	6293.7668	6294.4892	6343.1756	374.9546	288.7362	26.0893
	SD 2	6270.1159	6271.7105	6344.3708	368.5360	282.5509	27.0558
	SD WS	6461.8271	6461.9663	6482.3146	1,062,506.0989	754.4205	95.6340
	SS	6588.5849	6589.0859	6629.8826	1,266,745.7849	635.2117	52.7323

Table 2. Cont.

Country	Model	AIC	AICc	BIC	MSE	MAE	MAPE
Jamaica	SD 1	4658.5020	4660.0741	4733.0297	97.2971	81.5668	38.4807
	SD 2	4704.6173	4705.3228	4754.3235	105.9428	89.4866	40.5211
	SD WS	4705.8447	4705.9785	4726.5435	18,850.7210	80.7728	42.7940
	SS	4837.9013	4838.4036	4879.1967	107,479.4776	171.1706	75.7571
Panama	SD 1	6569.8656	6571.4378	6644.3934	134.0009	108.6573	21.8896
	SD 2	6571.3742	6572.0812	6621.0594	136.3494	110.4343	22.2704
	SD WS	6850.5974	6850.7311	6871.2995	42,451.3021	139.0089	28.3498
	SS	6222.0811	6222.6217	6262.5795	28,495.6600	111.9751	22.9152
Uruguay	SD 1	4884.0880	4884.7952	4933.7672	329.8169	271.7384	24.2383
	SD 2	4784.3311	4785.9033	4858.8589	320.9517	261.6523	23.6438
	SD WS	4842.6633	4842.7969	4863.3720	335,154.0779	292.6989	28.2122
	SS	4737.7469	4738.2430	4779.1512	298,958.1937	279.8100	26.9180

Table 3. AIC, AICc, BIC, and loss functions (forecasting window: last 14 days).

Country	Model	AIC	AICc	BIC	MSE	MAE	MAPE
Argentina	SD 1	8175.2700	8176.8691	8249.5185	3197.9468	2639.5945	24.1452
	SD 2	8271.6612	8272.3811	8321.1430	3371.1225	2809.3709	25.2801
	SD WS	8406.7033	8406.8398	8427.3150	49,140,353.3414	4196.7107	45.3911
	SS	8379.6315	8380.1359	8420.8807	18,184,571.1667	2578.3910	30.0359
Brazil	SD 1	8647.7178	8649.3169	8721.9664	2894.9226	2384.5114	25.6791
	SD 2	8637.4367	8638.1589	8686.8794	3065.6126	2554.0550	27.6030
	SD WS	8838.0213	8838.1575	8858.6376	30,982,304.8005	3506.3766	43.2434
	SS	8876.8100	8877.3134	8918.0787	26,819,716.2958	3169.0974	36.5192
Chile	SD 1	6900.4569	6902.0560	6974.7054	569.6145	462.6948	16.1672
	SD 2	6947.1479	6947.8681	6996.6269	570.1986	467.3224	16.1924
	SD WS	7382.4926	7382.6286	7403.1159	1,067,731.3998	735.1098	26.8141
	SS	6994.4527	6994.9572	7035.7019	691,370.5675	583.3890	24.0062
Colombia	SD 1	7636.0628	7637.6619	7710.3113	2041.0238	1760.6786	19.5618
	SD 2	7644.9216	7645.6422	7694.3920	2020.2438	1731.1616	19.1392
	SD WS	7739.3255	7739.4618	7759.9365	10,868,589.6806	1987.7646	21.5616
	SS	7719.2850	7719.7895	7760.5342	11,493,721.1180	2106.8066	26.9954
Cuba	SD 1	5087.1428	5088.7419	5161.3913	685.2727	601.0140	24.4800
	SD 2	5155.6897	5156.4089	5205.1788	961.0687	857.5462	27.9208
	SD WS	5086.2412	5086.3770	5106.8676	2,245,995.6206	723.6386	23.9827
	SS	4933.7971	4934.3016	4975.0463	1,476,321.3263	707.0039	37.1587
Guatemala	SD 1	6274.8259	6276.4240	6349.0671	432.2001	322.0076	33.8236
	SD 2	6344.1386	6344.8575	6393.6230	439.7635	333.0616	35.3578
	SD WS	6231.7189	6231.8619	6252.0626	1,238,553.6801	831.8914	93.8069
	SS	6396.6383	6397.1523	6437.6775	2,093,344.2267	826.1275	64.7631
Jamaica	SD 1	4577.2449	4578.8440	4651.4934	127.0198	106.1333	45.8103
	SD 2	4627.4318	4628.1483	4676.9655	136.2133	114.0903	47.4340
	SD WS	4634.5638	4634.6997	4655.1884	29,838.2604	101.3054	49.0764
	SS	5202.6202	5203.0954	5244.4736	138,632.3748	187.4398	76.6255

Table 3. Cont.

Country	Model	AIC	AICc	BIC	MSE	MAE	MAPE
Panama	SD 1	6470.3736	6471.9727	6544.6222	150.5995	119.7430	25.3388
	SD 2	6471.8290	6472.5479	6521.3280	153.2067	121.4780	25.5953
	SD WS	6703.3882	6703.5243	6724.0094	45,059.8159	148.5483	30.9317
	SS	5994.4678	5995.0285	6034.6011	49,498.3959	149.1045	29.7651
Uruguay	SD 1	4739.2554	4740.8554	4813.4939	392.8616	322.5024	28.8932
	SD 2	4843.9065	4844.6268	4893.3837	409.2816	334.2830	31.5082
	SD WS	4806.4207	4806.5566	4827.0487	426,375.0069	351.6242	33.1181
	SS	4649.3840	4649.8886	4690.6331	494,822.8223	369.7121	37.6505

Table 4. AIC, AICc, BIC, and loss functions (forecasting window: last 28 days).

Country	Model	AIC	AICc	BIC	MSE	MAE	MAPE
Argentina	SD 1	7933.59216	7935.2480	8007.2728	5189.7655	4219.0258	36.2552
	SD 2	8046.926927	8047.6706	8096.0505	5367.0909	4366.9248	38.2809
	SD WS	8136.394036	8136.5355	8156.8363	82,370,566.8139	5322.1663	54.2638
	SS	8088.467599	8088.9933	8129.3335	32,170,702.1469	3753.4018	44.5420
Brazil	SD 1	8396.9131	8398.5706	8470.5747	4007.0473	3318.6124	37.0109
	SD 2	8384.3370	8385.0852	8433.3866	4134.1578	3442.6450	38.8869
	SD WS	8534.4407	8534.5821	8554.8778	42,251,093.3462	4151.6625	49.4397
	SS	8536.3283	8536.8557	8577.1623	75,839,238.9418	5397.3759	55.1246
Chile	SD 1	6758.694984	6760.3524	6832.3550	996.1884	805.6067	26.8196
	SD 2	6760.079588	6760.8265	6809.1586	1012.6425	820.0937	27.3999
	SD WS	7130.248944	7130.3902	7150.6921	2,689,008.2871	1070.7300	37.1054
	SS	6788.432479	6788.9545	6829.3637	1,681,886.1884	908.0762	40.4911
Colombia	SD 1	7409.855313	7411.5113	7483.5314	3857.9707	3264.2294	36.3053
	SD 2	7429.951682	7430.6957	7479.0645	3636.0051	3041.9816	33.2373
	SD WS	7507.145544	7507.2866	7527.5960	31,129,971.4861	3367.9660	36.2210
	SS	7477.488416	7478.0112	7518.4103	28,223,384.5131	3245.6306	41.7716
Cuba	SD 1	4850.0780	4851.7383	4923.7095	1008.8684	861.4322	35.6252
	SD 2	4942.4274	4943.1732	4991.5171	1236.3509	1068.8652	40.0612
	SD WS	4849.2351	4849.3760	4869.6902	4,131,481.9817	968.8769	36.2243
	SS	4244.8179	4245.3741	4285.0725	3,133,873.0682	1062.5131	39.7491
Guatemala	SD 1	6034.6615	6036.3211	6108.2611	604.4476	463.1176	44.4914
	SD 2	6058.5938	6059.3445	6107.5678	592.5558	454.5504	39.5764
	SD WS	6013.4898	6013.6373	6033.6838	1,449,870.5471	912.3629	92.5962
	SS	8798.9832	8799.3545	8843.0131	134,451.6239	232.2018	97.9899
Jamaica	SD 1	4345.2526	4346.9332	4418.6825	146.7090	119.2289	57.5685
	SD 2	4451.0057	4451.7509	4500.1125	143.1995	114.7898	53.4278
	SD WS	4531.9877	4532.1268	4552.5144	35,160.6978	105.0457	51.1179
	SS	6034.1902	6034.5985	6077.3523	65,056.8814	130.9791	91.3099
Panama	SD 1	6273.7113	6275.3673	6347.3874	192.1973	151.0401	30.7112
	SD 2	6274.8232	6275.5673	6323.9407	194.7002	153.1452	31.1234
	SD WS	6403.5157	6403.6567	6423.9690	60,999.7748	175.9676	35.3154
	SS	5635.3098	5635.9036	5674.8490	105,743.2413	210.5126	41.5893

Table 4. Cont.

Country	Model	AIC	AICc	BIC	MSE	MAE	MAPE
Uruguay	SD 1	4509.681247	4511.3419	4583.3386	528.6854	426.8793	38.0930
	SD 2	4635.014697	4635.7589	4684.1502	512.4454	415.3082	38.3145
	SD WS	4568.527711	4568.6686	4588.9937	777,495.0436	454.9869	41.2574
	SS	4464.8041	4465.3277	4505.7387	734,336.1219	430.1770	39.5965

4. Conclusions

In this paper, we apply new score-driven and state-space models for the negative binomial distribution for new cases of infection with COVID-19 to a specific dataset of nine Latin American countries. We use daily data for the period of 1 April 2020 to 31 December 2021 and control for weekly seasonal effects in new cases of infection with COVID-19. We use the same econometric specifications for these countries, because they have similar geographical and social structures.

The in-sample model fits and out-of-sample forecasting performances of alternative models for predicting the number of new COVID-19 infections are compared. Assuming that data are generated by the negative binomial distribution, the predictive accuracies of (i) different specifications of score-driven models and (ii) a nonlinear state-space model with unobserved components are analyzed. We extend the relevant literature on score-driven models by considering a weekly seasonality component for the daily COVID-19 observations for both (i) and (ii) and the use of the negative binomial distribution for (ii).

We find that the score-driven model provides the most accurate forecast of COVID-19 cases. This has the potential to motivate the future use of score-driven models for forecasting daily cases during pandemics. The novel statistical models of the present work may be used by authorities to decide on alternative actions, such as quarantines and vaccination processes, to control the current COVID-19 or other future pandemics.

Our results are robust as we find that the forecasting performance of the score-driven model is superior to that of the nonlinear state-space model with unobserved components for all countries. For the sociocultural context of Latin American countries, the score-driven models for forecasting new cases of infection with COVID-19 seem to work well. A scientific implication of our paper is the potential future use of the new score-driven models for forecasting new COVID-19 cases for other countries.

The limitations of our paper include the use of the negative binomial distribution and the specific dataset for nine Latin American countries for which data are available for us. Future work may consider other score-driven discrete probability distributions as alternatives to the score-driven negative binomial distribution. Moreover, future work may use a more complete dataset that includes further Latin American countries.

Author Contributions: Conceptualization, S.C.-E. and F.N.-M.; methodology, S.C.-E., S.B. and F.N.-M.; software, P.V. and F.N.-M.; validation, C.C.-C. and S.B.; data creation, C.C.-C. and P.V.; writing—original draft preparation, S.C.-E. and P.V.; writing—review and editing, S.B., C.C.-C. and F.N.-M. All authors have read and agreed to the published version of the manuscript.

Funding: Contreras-Espinoza's research was fully supported by Proyecto Regular DIUBB 190908244 3/R of the Universidad del Bío-Bío. Novoa-Muñoz's research was fully supported by project 2220529 IF/R and Fondo de Apoyo a la Participación a Eventos Internacionales (FAPEI) at Universidad del Bío-Bío, Chile. Blazsek gratefully acknowledges research funding from Universidad Francisco Marroquín. Caamaño-Carrillo's research was funded by FONDECYT (Chile) grant No. 11220066 and by Proyecto Regular DIUBB 2120538 IF/R de la Universidad del Bío-Bío.

Institutional Review Board Statement: Not applicable.

Informed Consent Statement: Not applicable.

Data Availability Statement: The COVID-19 data set was taken from the COVID-19 Data Repository of the Center for Systems Science and Engineering (CSSE) at Johns Hopkins University.

Conflicts of Interest: The authors declare no conflict of interest.

Abbreviations

ANFIS	Adaptive neuro-fuzzy inference system
AIC	Akaike information criterion
AICc	Corrected Akaike information criterion
AIDS	Acquired immune deficiency syndrome
ADF	Augmented Dickey–Fuller
ARIMA	Autoregressive integrated moving average
AI	Artificial intelligence
SARIMA	Seasonal ARIMA
BC	Before Christ
BIC	Bayesian information criterion
COVID-19	Coronavirus disease 2019
CSSE	Center for Systems Science and Engineering
DCS	Dynamic conditional score
DGP	Data generating process
DL	Deep learning
GAS	Generalized autoregressive score
HIV	Human immunodeficiency virus
JB	Jarque–Bera
LL	Log-likelihood
LSTM	Long short-term memory
MAPE	Mean Absolute Percentage Error
MAE	Mean Absolute Error
MSE	Mean Square Error
PCR	Polymerase chain reaction
Sars-CoV-2	Severe acute respiratory syndrome coronavirus 2
SDev	Standard deviation
SD 1	Score-driven 1
SD 2	Score-driven 2
SD WS	Score-driven, without seasonality
SS	State space
SEIR	Susceptible, exposed, infected, and recovered
SIR	Susceptible, infected, recovered
SIRD	SIR deceased

Appendix A

Table A1. COVID-19 forecasting models from the literature.

Forecasting Model	Citation
Adaptive neuro-fuzzy inference system (ANFIS)	[36]
Artificial intelligence (AI)	[37]
Autoregressive integrated moving average (ARIMA) model	[38–42]
Ecological Niche models	[43]
Flower pollination algorithm	[36]
Genetic programming	[41,42,44–46]
Hybrid approaches that include ARIMA and wavelet model	[40,41]
Iteration method	[47]
Logistic growth model	[48–50]
Long short-term memory (LSTM) network	[51]
Machine learning	[52]
Models based on growth curves	[20]
Moving average (MA) model	[53]
Neural network	[42,54]

Table A1. *Cont.*

Forecasting Model	Citation
Phenomenological model	[55]
Polynomial neural network	[56]
Predictive models based on the Gompertz curves	[57]
Prophet algorithm	[58]
Random forest	[52]
Regression methods	[52,59–61]
Regression tree algorithm	[40]
SARIMA (seasonal ARIMA) model	[62]
Support vector Kuhn–Tucker	[63]
Support vector machine	[52,56,63]
Susceptible, exposed, infected, and recovered (SEIR)	[64,65]
Susceptible, infected, recovered (SIR) model	[66,67]
Susceptible, infected, recovered, and deceased (SIRD)	[68,69]
SutteARIMA method	[70]

Appendix B

Table A2. Parameter estimates for Argentina.

	SD 1	SD 2	SD WS	SS
κ_1	0.4810 *** (0.0250)	0.4245 *** (0.0422)	0.6822 *** (0.0738)	NA
κ_2	0.0563 *** (0.0111)	0.0387 *** (0.0093)	0.0178 (0.0111)	NA
κ_{Monday}	0.0530 *** (0.0166)	0.1499 *** (0.0301)	NA	NA
κ_{Tuesday}	0.2202 *** (0.0141)	NA	NA	NA
$\kappa_{\text{Wednesday}}$	0.0191 (0.0268)	NA	NA	NA
κ_{Thursday}	0.4169 *** (0.0861)	NA	NA	NA
κ_{Friday}	0.0000 (0.0165)	NA	NA	NA
κ_{Saturday}	0.3287 * (0.1779)	NA	NA	NA
κ_{Sunday}	0.1711 *** (0.0455)	NA	NA	NA
ν	13.6133 *** (0.8289)	12.9432 *** (0.7937)	6.6132 *** (0.3795)	NA
σ_{δ}^2	NA	NA	NA	0.0092 *** (0.0002)
σ_{β}^2	NA	NA	NA	0.0049 *** (0.0004)
σ_{γ}^2	NA	NA	NA	0.0003 (0.0005)

Notes: Standard deviations are in parentheses. *** and * is parameter significance at the 1% and 10% levels, respectively. For SD 2, $\kappa_j = \kappa_{\text{Monday},t}$ for $j = \text{Tuesday}, \dots, \text{Sunday}$.

Table A3. Parameter estimates for Brazil.

	SD 1	SD 2	SD WS	SS
κ_1	0.6955 *** (0.0445)	0.6792 *** (0.0488)	0.7908 *** (0.0462)	NA
κ_2	0.0155 ** (0.0070)	0.0142 (0.0088)	0.0000 (0.0008)	NA
κ_{Monday}	0.0000 (0.0307)	0.0598 *** (0.0109)	NA	NA
κ_{Tuesday}	0.0248 (0.0185)	NA	NA	NA
$\kappa_{\text{Wednesday}}$	0.0000 (0.0223)	NA	NA	NA
κ_{Thursday}	0.0000 (0.0246)	NA	NA	NA
κ_{Friday}	0.0000 (0.0227)	NA	NA	NA
κ_{Saturday}	0.1071 ** (0.0525)	NA	NA	NA
κ_{Sunday}	0.1815 *** (0.0492)	NA	NA	NA
ν	13.8207 *** (0.7742)	13.2981 *** (0.7523)	7.3978 *** (0.4104)	NA
σ_{δ}^2	NA	NA	NA	0.0205 *** (0.0002)
σ_{β}^2	NA	NA	NA	0.0143 *** (0.0002)
σ_{γ}^2	NA	NA	NA	0.0001 (0.0006)

Notes: Standard deviations are in parentheses. *** and ** is parameter significance at the 1% and 5% levels, respectively. For SD 2, $\kappa_j = \kappa_{\text{Monday},t}$ for $j = \text{Tuesday}, \dots, \text{Sunday}$.

Table A4. Parameter estimates for Chile.

	SD 1	SD 2	SD WS	SS
κ_1	0.3536 *** (0.0312)	0.3265 *** (0.0290)	0.1373 *** (0.0166)	NA
κ_2	0.0508 *** (0.0062)	0.0480 *** (0.0058)	0.0381 *** (0.0037)	NA
κ_{Monday}	0.2165 *** (0.0763)	0.2599 *** (0.0298)	NA	NA
κ_{Tuesday}	0.2138 *** (0.0689)	NA	NA	NA
$\kappa_{\text{Wednesday}}$	0.1546 *** (0.0478)	NA	NA	NA
κ_{Thursday}	0.0000 (0.0190)	NA	NA	NA
κ_{Friday}	0.0097 (0.0162)	NA	NA	NA
κ_{Saturday}	0.5496 *** (0.0784)	NA	NA	NA
κ_{Sunday}	0.3805 *** (0.0984)	NA	NA	NA
v	39.9089 *** (2.2882)	37.1677 *** (0.0171)	13.1141 *** (0.0218)	NA
σ_δ^2	NA	NA	NA	0.0046 *** (0.0002)
σ_β^2	NA	NA	NA	0.0013 * (0.0006)
σ_γ^2	NA	NA	NA	0.0002 (0.0005)

Notes: Standard deviations are in parentheses. *** and * is parameter significance at the 1% and 10% levels, respectively. For SD 2, $\kappa_j = \kappa_{\text{Monday},t}$ for $j = \text{Tuesday}, \dots, \text{Sunday}$.

Table A5. Parameter estimates for Colombia.

	SD 1	SD 2	SD WS	SS
κ_1	0.6284 *** (0.0450)	0.5723 *** (0.0449)	0.7356 *** (0.0455)	NA
κ_2	0.0356 *** (0.0073)	0.0512 *** (0.0094)	0.0000 *** (0.0004)	NA
κ_{Monday}	0.1836 *** (0.0534)	0.0000 (0.0287)	NA	NA
κ_{Tuesday}	0.0000 (0.0147)	NA	NA	NA
$\kappa_{\text{Wednesday}}$	0.0000 (0.0185)	NA	NA	NA
κ_{Thursday}	0.1300 *** (0.0385)	NA	NA	NA
κ_{Friday}	0.0000 (0.0177)	NA	NA	NA
κ_{Saturday}	0.0264 * (0.0152)	NA	NA	NA
κ_{Sunday}	0.1600 *** (0.0417)	NA	NA	NA
v	42.4229 *** (0.0263)	42.5514 *** (2.4817)	33.0859 *** (1.9223)	NA
σ_δ^2	NA	NA	NA	0.0006 *** (0.0002)
σ_β^2	NA	NA	NA	0.0005 * (0.0003)
σ_γ^2	NA	NA	NA	0.0000 (0.0211)

Notes: Standard deviations are in parentheses. *** and * is parameter significance at the 1% and 10% levels, respectively. For SD 2, $\kappa_j = \kappa_{\text{Monday},t}$ for $j = \text{Tuesday}, \dots, \text{Sunday}$.

Table A6. Parameter estimates for Cuba.

	SD 1	SD 2	SD WS	SS
κ_1	0.4972 *** (0.0373)	0.5128 *** (0.0391)	0.4451 *** (0.0450)	NA
κ_2	0.0074 *** (0.0024)	0.0094 *** (0.0036)	0.0131 * (0.0071)	NA
κ_{Monday}	0.0000 (0.0142)	0.0180 (0.0110)	NA	NA
κ_{Tuesday}	0.0192 * (0.0116)	NA	NA	NA
$\kappa_{\text{Wednesday}}$	0.0000 (0.0170)	NA	NA	NA
κ_{Thursday}	0.0000 (0.0143)	NA	NA	NA
κ_{Friday}	0.0116 (0.0171)	NA	NA	NA
κ_{Saturday}	0.0000 (0.0222)	NA	NA	NA
κ_{Sunday}	0.0757 *** (0.0272)	NA	NA	NA
v	17.7669 *** (1.3024)	18.6270 *** (1.4951)	18.7317 *** (1.5171)	NA
σ_δ^2	NA	NA	NA	0.0162 *** (0.0002)
σ_β^2	NA	NA	NA	0.0087 *** (0.0004)
σ_γ^2	NA	NA	NA	0.0001 (0.0020)

Notes: Standard deviations are in parentheses. *** and * is parameter significance at the 1% and 10% levels, respectively. For SD 2, $\kappa_j = \kappa_{\text{Monday},t}$ for $j = \text{Tuesday}, \dots, \text{Sunday}$.

Table A7. Parameter estimates for Guatemala.

	SD 1	SD 2	SD WS	SS
κ_1	0.2173 *** (0.0257)	0.2454 *** (0.0262)	0.1447 *** (0.0265)	NA
κ_2	0.0075 ** (0.0031)	0.0000 (0.0215)	0.0028 ** (0.0012)	NA
κ_{Monday}	0.2426 *** (0.0480)	0.1443 *** (0.0215)	NA	NA
κ_{Tuesday}	0.1587 *** (0.0615)	NA	NA	NA
$\kappa_{\text{Wednesday}}$	0.0907 ** (0.0421)	NA	NA	NA
κ_{Thursday}	0.0358 (0.0452)	NA	NA	NA
κ_{Friday}	0.0440 (0.0295)	NA	NA	NA
κ_{Saturday}	0.0000 (0.0176)	NA	NA	NA
κ_{Sunday}	0.1493 ** (0.0585)	NA	NA	NA
v	5.4384 *** (0.3232)	5.2768 *** (0.3325)	2.0380 *** (0.1097)	NA
σ_δ^2	NA	NA	NA	0.1427 *** (0.0002)
σ_β^2	NA	NA	NA	0.09732 *** (0.0009)
σ_γ^2	NA	NA	NA	0.0035 *** (0.0005)

Notes: Standard deviations are in parentheses. *** and ** is parameter significance at the 1% and 5% levels, respectively. For SD 2, $\kappa_j = \kappa_{\text{Monday},t}$ for $j = \text{Tuesday}, \dots, \text{Sunday}$.

Table A8. Parameter estimates for Jamaica.

	SD 1	SD 2	SD WS	SS
κ_1	0.1906 *** (0.0218)	0.1860 *** (0.0238)	0.1901 *** (0.0247)	NA
κ_2	0.0186 *** (0.0032)	0.0178 *** (0.0030)	0.0177 *** (0.0030)	NA
κ_{Monday}	0.0000 (0.0146)	0.0000 (0.0118)	NA	NA
κ_{Tuesday}	0.0692 * (0.0400)	NA	NA	NA
$\kappa_{\text{Wednesday}}$	0.0000 (0.0293)	NA	NA	NA
κ_{Thursday}	0.0000 (0.0137)	NA	NA	NA
κ_{Friday}	0.0000 (0.0216)	NA	NA	NA
κ_{Saturday}	0.0493 (0.0303)	NA	NA	NA
κ_{Sunday}	0.0000 (0.0207)	NA	NA	NA
v	2.4836 *** (0.1558)	2.4600 *** (0.1557)	2.3768 *** (0.1501)	NA
σ_δ^2	NA	NA	NA	0.1025 *** (0.0005)
σ_β^2	NA	NA	NA	0.0284 *** (0.0001)
σ_γ^2	NA	NA	NA	0.0506 *** (0.0006)

Notes: Standard deviations are in parentheses. *** and * is parameter significance at the 1% and 10% levels, respectively. For SD 2, $\kappa_j = \kappa_{\text{Monday},t}$ for $j = \text{Tuesday}, \dots, \text{Sunday}$.

Table A9. Parameter estimates for Panama.

	SD 1	SD 2	SD WS	SS
κ_1	0.1515 *** (0.0281)	0.1523 *** (0.0284)	0.1354 *** (0.0273)	NA
κ_2	0.0186 *** (0.0048)	0.0185 *** (0.0048)	0.0171 *** (0.0040)	NA
κ_{Monday}	0.0746 * (0.0451)	0.0453 *** (0.0165)	NA	NA
κ_{Tuesday}	0.0486 (0.0410)	NA	NA	NA
$\kappa_{\text{Wednesday}}$	0.0403 (0.0377)	NA	NA	NA
κ_{Thursday}	0.0000 (0.0107)	NA	NA	NA
κ_{Friday}	0.0000 (0.0145)	NA	NA	NA
κ_{Saturday}	0.0000 (0.0081)	NA	NA	NA
κ_{Sunday}	0.0853 (0.0648)	NA	NA	NA
v	2.9190 *** (0.1732)	2.8883 *** (0.1730)	2.6564 *** (0.1569)	NA
σ_δ^2	NA	NA	NA	0.0150 *** (0.0003)
σ_β^2	NA	NA	NA	0.0089 *** (0.0005)
σ_γ^2	NA	NA	NA	0.4780 *** (0.0001)

Notes: Standard deviations are in parentheses. *** and * is parameter significance at the 1% and 10% levels, respectively. For SD 2, $\kappa_j = \kappa_{\text{Monday},t}$ for $j = \text{Tuesday}, \dots, \text{Sunday}$.

Table A10. Parameter estimates for Uruguay.

	SD 1	SD 2	SD WS	SS
κ_1	0.3761 *** (0.0224)	0.3810 *** (0.0219)	0.3202 *** (0.0217)	NA
κ_2	0.0106 *** (0.0020)	0.0110 *** (0.0027)	0.0136 *** (0.0032)	NA
κ_{Monday}	0.0000 (0.0240)	0.0537 *** (0.0115)	NA	NA
κ_{Tuesday}	0.0519 * (0.0302)	NA	NA	NA
$\kappa_{\text{Wednesday}}$	0.0000 (0.0183)	NA	NA	NA
κ_{Thursday}	0.0350 (0.0225)	NA	NA	NA
κ_{Friday}	0.0499 *** (0.0147)	NA	NA	NA
κ_{Saturday}	0.0000 (0.0161)	NA	NA	NA
κ_{Sunday}	0.1108 *** (0.0220)	NA	NA	NA
ν	13.8626 *** (1.0409)	12.7228 *** (0.9896)	9.6245 *** (0.0136)	NA
σ_{δ}^2	NA	NA	NA	0.0186 *** (0.0002)
σ_{β}^2	NA	NA	NA	0.0949 *** (0.0004)
σ_{γ}^2	NA	NA	NA	0.0002 (0.0008)

Notes: Standard deviations are in parentheses. *** and * is parameter significance at the 1% and 10% levels, respectively. For SD 2, $\kappa_j = \kappa_{\text{Monday},t}$ for $j = \text{Tuesday}, \dots, \text{Sunday}$.

References

- Barrado, D. Vivimos un Punto de Inflexión: La Generación 2020 y la Nueva Sociedad. 2020. Available online: <https://telos.fundaciontelefonica.com/punto-de-inflexion-la-generacion-2020-y-la-nueva-sociedad/> (accessed on 1 December 2022).
- Norrie, P. *A History of Disease in Ancient Times: More Lethal than War*; Springer Nature: Berlin/Heidelberg, Germany, 2016.
- Zietz, B.P.; Dunkelberg, H. The History of the Plague and the Research on the Causative Agent *Versinia Pestis*. *Int. J. Hyg. Envir. Heal.* **2004**, *207*, 165–178. [CrossRef] [PubMed]
- Guerra, F. Origen de las Epidemias en la Conquista de América. *Quinto Centen.* **1998**, *14*, 43–51.
- López, S.; Garrido, F.; Hernández, M. Desarrollo Histórico de la Epidemiología: Su Formación Como Disciplina Científica. *Salud Pública de México* **2000**, *42*, 133–143. [CrossRef]
- González, B.; Tomaino, L.; Serra, L.; Barber, Rodríguez, P. -Mireles, S. COVID-19: Pandemia de Modelos Matemáticos. 2020. Available online: <https://theconversation.com/covid-19-pandemia-de-modelos-matematicos-136212> (accessed on 1 December 2022).
- Grillo-Ardila, E.K.; Santaella-Tenorio, J.; Guerrero, R.; Bravo, L.E. Mathematical Model and COVID-19. *Colomb. Méd.* **2020**, *51*, 1–9.
- Creal, D.; Koopman, S.J.; Lucas, A. A General Framework for Observation Driven Time-Varying Parameter Models. Tinbergen Institute Discussion Paper 08-108/4. 2008. Available online: <https://papers.tinbergen.nl/08108.pdf> (accessed on 1 December 2022).
- Harvey, A.C.; Chakravarty, T. Beta-t-EGARCH. *Cambridge Working Paper in Economics, CWPE 0840*. 2008. Available online: <https://www.econ.cam.ac.uk/research-files/repec/cam/pdf/cwpe0840.pdf> (accessed on 1 December 2022).
- Cox, D.R. Statistical Analysis of Time Series: Some Recent Developments. *Scand. J. Stat.* **1981**, *8*, 93–115.
- Harvey, A. *Dynamic Models for Volatility and Heavy Tails: With Applications to Financial and Economic Time Series (Econometric Society Monographs)*; Cambridge University Press: Cambridge, UK, 2013.
- Blazsek, S.; Licht, A. Dynamic Conditional Score Models: A Review of Their Applications. *Appl. Econ.* **2020**, *52*, 1181–1199. [CrossRef]
- Creal, D.; Koopman, S.J.; Lucas, A. Generalized Autoregressive Score Models with Applications. *J. Appl. Econom.* **2013**, *28*, 777–795. [CrossRef]
- Blasques, F.; Koopman, S.J.; Lasak, K.; Lucas, A. In-Sample Confidence Bands and Out-of-Sample Forecast Bands for Time-Varying Parameters in Observation-Driven Models. *Int. J. Forecast.* **2016**, *32*, 875–887. [CrossRef]
- Blasques, F.; van Brummelen, J.; Koopman, S.J.; Lucas, A. Maximum Likelihood Estimation for Score-Driven Models. *J. Econom.* **2022**, *227*, 325–346. [CrossRef]
- Harvey, A.; Luati, A. Filtering With Heavy Tails. *J. Am. Stat. Assoc.* **2014**, *109*, 1112–1122 [CrossRef]
- Creal, D.; Koopman, S.J.; Lucas, A. A Dynamic Multivariate Heavy-Tailed Model for Time-Varying Volatilities and Correlations. *J. Bus. Econ. Stat.* **2011**, *29*, 552–563 [CrossRef]
- Caivano, M.; Harvey, A. Time-Series Models with an EGB2 Conditional Distribution. *J. Time Ser. Anal.* **2014**, *35*, 558–571 [CrossRef]
- Contreras, S.; Caamaño-Carrillo, C.; Contreras-Reyes, J. Generalized Autoregressive Score Models Based on Sinh-Arcsinh Distributions for Time Series Analysis. *J. Comput. Appl. Math.* **2022**. *in press*.
- Harvey, A.C.; Kattuman, P. Time Series Models Based on Growth Curves with Applications to Forecasting Coronavirus. In *Harvard Data Science Review, Special Issue 1—COVID-19*; MIT Press: Cambridge, MA, USA, 2020; pp. 1–39.
- Harvey, A.; Lit, R. Coronavirus and the Score-Driven Negative Binomial Distribution. *Time Series Lab—Article Series*. 2020. Available online: <https://www.timeserieslab.com/articles/negbin.pdf> (accessed on 1 December 2022).
- Ayala, A.; Blazsek, S.; Licht, A. Score-Driven Stochastic Seasonality of the Russian Rouble: An Application Case Study for the Period of 1999 to 2020. *Empir. Econ.* **2022**, *62*, 2179–2203. [CrossRef]
- Blazsek, S.; Escribano, A.; Licht, A. Multivariate Markov-Switching Score-Driven Models: An Application to the Global Crude Oil Market. *Stud. Nonlinear Dyn. E* **2022**, *26*, 313–335. [CrossRef]

24. Ayala, A.; Blazsek, S. Score-Driven Models of Stochastic Seasonality in Location and Scale: An Application Case Study of the Indian Rupee to USD Exchange Rate. *Appl. Econ.* **2019**, *51*, 4083–4103. [[CrossRef](#)]
25. Ayala, A.; Blazsek, S. Score-Driven Currency Exchange Rate Seasonality as Applied to the Guatemalan Quetzal/US Dollar. *SERIEs* **2019**, *10*, 65–92. [[CrossRef](#)]
26. Caivano, M.; Harvey, A.; Luati, A. Robust Time Series Models with Trend and Seasonal Components. *SERIEs* **2016**, *7*, 99–120. [[CrossRef](#)]
27. Harvey, A.C. *Forecasting, Structural Time Series Models and the Kalman Filter*; Cambridge University Press: Cambridge, UK, 1990.
28. Harvey, A.C.; Shephard, N. Structural Time Series Models. In *Handbook of Statistics; Econometrics*; Maddala, G.S., Rao, C.R., Vinod, H.D., Eds.; Elsevier: Amsterdam, The Netherlands, 1993; Volume 11; pp. 261–302.
29. Commandeur, J.J.; Koopman, S.J. *An Introduction to State Space Time Series Analysis*; Oxford University Press: Oxford, UK, 2007.
30. Durbin, J.; Koopman, S.J. In *Time Series Analysis by State Space Methods*; Oxford University Press: Oxford, UK, 2012.
31. Helske, J.; Helske, M.J.; Suggests, M.A. CRAN Package KFAS. 2021. Available online: <https://cran.r-project.org/web/packages/KFAS/index.html> (accessed on 1 December 2022).
32. Gavilán, A. Tecnología Médica Que Verificó Muestra de Coronavirus en Chile. Available online: <https://www.biobiochile.cl/noticias/nacional/region-del-maule/2020/03/03/angelica-gavilan-tecnologa-que-verifico-muestra-de-coronavirus-en-chile-no-lo-podia-creer.shtml> (accessed on 1 December 2022).
33. COVID-19 Data Repository by the Center for Systems Science and Engineering (CSSE) at Johns Hopkins University. Available online: <https://coronavirus.jhu.edu/map.html> (accessed on 1 December 2022).
34. Jarque, C.M.; Bera, A.K. Efficient Tests for Normality, Homoscedasticity and Serial Independence of Regression Residuals. *Econ. Lett.* **1980**, *6*, 255–259. [[CrossRef](#)]
35. Dickey, D.A.; Fuller, W.A. Distribution of the Estimators for Autoregressive Time Series with a Unit Root. *J. Am. Stat. Assoc.* **1979**, *74*, 427–431.
36. Al-qaness, M.A.A.; Ewees, A.A.; Fan, H.; Abd El Aziz, M. Optimization Method for Forecasting Confirmed Cases of COVID-19 in China. *J. Clin. Med.* **2020**, *9*, 674. [[CrossRef](#)]
37. Naudé, W. Artificial Intelligence against COVID-19: An Early Review. IZA Discussion Paper No. 13110. 2020. Available online: <https://ssrn.com/abstract=3568314> (accessed on 1 December 2022).
38. Dehesh, T.; Mardani-Fard, H.A.; Dehesh, P. Forecasting of COVID-19 Confirmed Cases in Different Countries with ARIMA Models. *MedRxiv*. 2020. Available online: <https://www.medrxiv.org/content/10.1101/2020.03.13.20035345v1> (accessed on 1 December 2022).
39. Chintalapudi, N.; Battineni, G.; Amenta, F. COVID-19 Virus Outbreak Forecasting of Registered and Recovered Cases after Sixty Day Lockdown in Italy: A Data Driven Model Approach. *J. Microbiol. Immunol. Infect.* **2020**, *53*, 396–403. [[CrossRef](#)]
40. Chakraborty, T.; Ghosh, I. Real-Time Forecasts and Risk Assessment of Novel Coronavirus (COVID-19) Cases: A Data-Driven Analysis. *Chaos Solitons Fractals* **2020**, *135*, 109850. [[CrossRef](#)]
41. Singh, S.; Singh Parmar, K.; Kumar, J.; Singh Makkhan, S.J. Development of New Hybrid Model of Discrete Wavelet Decomposition and Autoregressive Integrated Moving Average (ARIMA) Models in Application to One Month Forecast the Casualties Cases of COVID-19. *Chaos Solitons Fractals* **2020**, *135*, 109866. [[CrossRef](#)] [[PubMed](#)]
42. Moftakhar, L.; Seif, M.; Safe, M.S. Exponentially Increasing Trend of Infected Patients with COVID-19 in Iran: A Comparison of Neural Network and ARIMA Forecasting Models. *Iran. J. Public Health* **2020**, *49*, 92–100. [[CrossRef](#)]
43. Ren, H.; Zhao, L.; Zhang, A.; Song, L.; Liao, Y.; Lu, W.; Cui, C. Early Forecasting of the Potential Risk Zones of COVID-19 in China's Megacities. *Sci. Total Environ.* **2020**, *729*, 138995. [[CrossRef](#)] [[PubMed](#)]
44. Salgotra, R.; Gandomi, M.; Gandomi, A.H. Time Series Analysis and Forecast of the COVID-19 Pandemic in India Using Genetic Programming. *Chaos Solitons Fractals* **2020**, *138*, 109945. [[CrossRef](#)] [[PubMed](#)]
45. Salgotra, R.; Gandomi, M.; Gandomi, A.H. Evolutionary Modelling of the COVID-19 Pandemic in Fifteen Most Affected Countries. *Chaos Solitons Fractals* **2020**, *140*, 110118. [[CrossRef](#)]
46. Salgotra, R.; Gandomi, A.H. Time Series Analysis of the COVID-19 Pandemic in Australia Using Genetic Programming. *Data Sci. COVID-19* **2021**, 399–411. [[CrossRef](#)]
47. Perc, M.; Gorisek Miksic, N.; Slavinec, M.; Stozer, A. Forecasting COVID-19. *Front. Phys.* **2020**, *8*, 127. 2020.00127. [[CrossRef](#)]
48. Chen, D.G.; Chen, X.G.; Chen, J.K. Reconstructing and Forecasting the COVID-19 Epidemic in the United States Using a 5-Parameter Logistic Growth Model. *Glob. Health Res. Policy* **2020**, *5*, 7. [[CrossRef](#)]
49. Li, Q.; Feng, W.; Quan, Y.H. Trend and Forecasting of the COVID-19 Outbreak in China. *J. Infect.* **2020**, *80*, 472–474. [[CrossRef](#)] [[PubMed](#)]
50. Qeadan, F.; Honda, T.; Gren, L.H.; Dailey-Provost, J.; Benson, L.S.; VanDerslice, J.A.; Porucznik, C.A.; Waters, A.B.; Lacey, S.; Shoaf, K. Naive Forecast for COVID-19 in Utah Based on the South Korea and Italy Models – The Fluctuation between Two Extremes. *Int. J. Environ. Res. Public Health* **2020**, *17*, 2750. [[CrossRef](#)] [[PubMed](#)]
51. Reddy Chimmula, V.K.; Zhang, L. Time Series Forecasting of COVID-19 Transmission in Canada Using LSTM Networks. *Chaos Solitons Fractals* **2020**, *135*, 109864. [[CrossRef](#)]
52. Dal Molin Ribeiro, M.H.; Gomes da Silva, R.; CoccoMariani, V.; dos SantosCoelho, L. Short-Term Forecasting COVID-19 Cumulative Confirmed Cases: Perspectives for Brazil. *Chaos Solitons Fractals* **2020**, *135*, 109853. [[CrossRef](#)] [[PubMed](#)]

53. Chaudhry, R.M.; Hanif, A.; Chaudhary, M.; Minhas, S.; Mirza, K.; Ashraf, T.; Gilani, S.A.; Kashif, M. Coronavirus Disease 2019 (COVID-19): Forecast of an Emerging Urgency in Pakistan. *Cureus* **2020**, *12*, 15. [[CrossRef](#)] [[PubMed](#)]
54. Tamang, S.K.; Singh, P.D.; Datta, B. Forecasting of Covid-19 Cases Based on Prediction Using Artificial Neural Network Curve Fitting Technique. *Glob. J. Environ. Sci. Manag.* **2020**, *6*, 53–64.
55. Roos, K.; Lee, Y.; Luo, R.; Kirpich, A.; Rothenberg, R.; Hyman, J.M.; Yan, P.; Chowell, G. Real-Time Forecasts of the COVID-19 Epidemic in China from February 5th to February 24th, 2020. *Infect. Dis. Model.* **2020**, *5*, 256–263. [[CrossRef](#)]
56. Fong, S.; Li, G.; Dey, N.; Crespo, R.G.; Herrera-Viedma, E. Finding an Accurate Early Forecasting Model from Small Dataset: A Case of 2019-nCoV Novel Coronavirus Outbreak. *Int. J. Interact. Multimed. Artif. Intell.* **2020**, *6*, 132–140. [[CrossRef](#)]
57. Sánchez-Villegas, P.; Daponte-Codina, A. Modelos Predictivos de la Epidemia de COVID-19 en España con Curvas de Gompertz. *Gac. Sanit.* **2020**. [[CrossRef](#)]
58. Abdulmajeed, K.; Adeleke, M.; Popoola, L.J.D. Online Forecasting of Covid-19 Cases in Nigeria Using Limited Data. *Data Brief* **2020**, *30*, 105683. [[CrossRef](#)]
59. Ji, D.; Zhang, D.; Xu, J.; Chen, Z.; Yang, T.; Zhao, P.; Chen, G.; Cheng, G.; Wang, Y.; Bi, J.; Tan, L.; Lau, G.; Qin, E. Prediction for Progression Risk in Patients with COVID-19 Pneumonia: The CALL Score. *Clin. Infect. Dis.* **2020**, *71*, 1393–1399. [[CrossRef](#)]
60. Sujath, R.; Chatterjee, J.M.; Hassani, A.E. A Machine Learning Forecasting Model for COVID-19 Pandemic in India. *Stoch. Environ. Res. Risk Assess.* **2020**, *34*, 959–972. [[CrossRef](#)] [[PubMed](#)]
61. Gallardo, D.I.; Bourguignon, M.; Gómez, Y.M.; Caamaño-Carrillo, C.; Venegas, O. Parametric Quantile Regression Models for Fitting Double Bounded Response with Application to COVID-19 Mortality Rate Data. *Mathematics* **2022**, *10*, 2249. [[CrossRef](#)]
62. Yadav, S.; Yadav, P.K. The Peak of COVID-19 in India. *medRxiv.* **2020**. [[CrossRef](#)]
63. Parbat, D.; Chakraborty, M. A Python Based Support Vector Regression Model for Prediction of COVID19 Cases in India. *Chaos Solitons Fractals* **2020**, *138*, 109942. [[CrossRef](#)] [[PubMed](#)]
64. Zhao, C.; Tepekule, B.; Criscuolo, N.G.; Wendel Garcia, P.D.; Hilty, M.P.; Risc-Icu Consortium Investigators In Switzerland; Fumeaux, T.; Van Boeckel, T. icumonitoring.ch: a Platform for Short-Term Forecasting of Intensive Care Unit Occupancy During the COVID-19 Epidemic in Switzerland. *Swiss. Med. Wkly.* **2020**, *150*, w20524.
65. Reno, C.; Lenzi, J.; Navarra, A.; Barelli, E.; Gori, D.; Lanza, A.; Valentini, R.; Tang, B.; Fantini, M.P. Forecasting COVID-19-Associated Hospitalizations under Different Levels of Social Distancing in Lombardy and Emilia-Romagna, Northern Italy: Results from an Extended SEIR Compartmental Model. *J. Clin. Med.* **2020**, *9*, 11. [[CrossRef](#)]
66. Putra, S.; Khozin Mutamar, Z. Estimation of Parameters in the SIR Epidemic Model Using Particle Swarm Optimization. *Am. J. Math. Comput. Model.* **2019**, *4*, 83–93. [[CrossRef](#)]
67. Dil, S.; Dil, N.; Maken, Z.H. COVID-19 Trends and Forecast in the Eastern Mediterranean Region with a Particular Focus on Pakistan. *Cureus* **2020**, *12*, e8582. [[CrossRef](#)]
68. Fanelli, D.; Piazza, F. Analysis and Forecast of COVID-19 Spreading in China, Italy and France. *Chaos Solitons Fractals* **2020**, *134*, 109761. [[CrossRef](#)]
69. Anastassopoulou, C.; Russo, L.; Tsakris, A.; Siettos, C. Data-Based Analysis, Modelling and Forecasting of the COVID-19 Outbreak. *PLoS ONE* **2020**, *15*, e0230405. [[CrossRef](#)] [[PubMed](#)]
70. Ahmar, A.S.; del Val, E.B. SutteARIMA: Short-Term Forecasting Method, a Case—COVID-19 and Stock Market in Spain. *Sci. Total Environ.* **2020**, *729*, 138883. [[CrossRef](#)] [[PubMed](#)]

Disclaimer/Publisher’s Note: The statements, opinions and data contained in all publications are solely those of the individual author(s) and contributor(s) and not of MDPI and/or the editor(s). MDPI and/or the editor(s) disclaim responsibility for any injury to people or property resulting from any ideas, methods, instructions or products referred to in the content.